

Equivalence of space and time-bins in DPS-QKD

Gautam Shaw*, Shyam Sridharan*, Shashank Ranu^{†*}, Foram Shingala*, Prabha Mandayam[†], and Anil Prabhakar*

*Department of Electrical Engineering, IIT Madras, Chennai, India

[†]Department of Physics, IIT Madras, Chennai, India

Abstract—Key generation efficiency, and security, in DPS-QKD improve with an increase in the number of path delays or time-bin superpositions. We demonstrate the implementation of superposition states using time-bins, and establish an equivalence with path-based superposition, thus yielding a simpler implementation of higher-order superposition states for differential phase-shift quantum key distribution (DPS-QKD). We set up DPS-QKD, over 105 km of single mode optical fiber, with a quantum bit error rate of less than 15% at a secure key rate of 2 kbps. With temporal guard bands, the QBER reduced to less than 10%, but with a 20% reduction in the key rate.

Index Terms—Quantum key distribution, differential phase, secure key, spatial superposition, time-bin superposition.

I. INTRODUCTION

Quantum key distribution (QKD) enables secure key exchange between authenticated users, Alice and Bob, by relying on two aspects of quantum mechanics, Heisenberg's uncertainty principle and the no-cloning theorem [1]. When an adversary, Eve, attempts to steal information from the quantum channel, she also inevitably introduces disturbances in the channel and reveals herself. Since the first proposal by Bennett and Brassard in 1984 [2], there have been a variety of QKD protocols, both proposed and implemented [3–6]. Long distance field demonstrations of QKD mostly use discrete variables, some with active stabilization to mitigate environmental fluctuations [7]. In Appendix A, we provide the reader with a quick summary of key rates and channel lengths for a few recent implementations of QKD.

This article aims to establish the equivalence between a spatial and temporal generation of a superposition state for use in a differential phase-shift quantum key distribution (DPS-QKD) system. DPS-QKD as proposed by Inoue et al., is simple to implement and robust against slowly varying environmental fluctuations [6, 8]. DPS-QKD uses a pair of phases $\Phi = \{0, \pi\}$ to generate non-orthogonal states that cannot be distinguished with absolute certainty using a single measurement [9]. A theoretical security proof of the DPS protocol, with single photons and weak coherent sources, was established under the assumption that Eve is restricted to individual attacks and also it was concluded that individual attacks are more powerful than sequential attacks [10, 11]. An efficient phase encoding quantum key generation scheme, with narrow band heralded photons, was proposed by Yan et al., where key

information is carried by the phase modulation directly on the single-photon temporal waveform [12, 13]. Time-bin qubits, composed of temporal modes with weak coherent sources, are effective constituents to build a robust and simple QKD system with a high secure key rate [14]. To increase the secure key rate, with minimum resources, researchers have used two-dimensional and four-dimensional QKD protocols with time-bin and phase encoding [15]. Dellantonio et al. proposed two equivalent high dimensional MDI-QKD methods: space and time-bin encoding, which uses space to encode information in different paths and time-slots to encode qudits [16]. In high dimensional QKD protocols, multiple bits of information are encoded on a single photon, hence, it increases the channel capacity and is more robust against channel noise.

The recently introduced round-robin differential phase-shift quantum key distribution (RR-DPS-QKD) scheme addresses the effects of environmental disturbances, and gives us an upper bound on our tolerance to error rates with a bit error rate as high as 29% [17]. But such schemes requires the addition of optical switches and delays that make Bob's set-up more complex [18].

In Sec. IV, we show that the two schemes, of spatial and temporal superposition, yield comparable key rates in kbps, with a QBER < 0.2 . However, time-bins are defined electronically, and are significantly easier to generate. The scheme does require more precise timing synchronization, and we have developed the means to characterize the photon arrival time at our detector to within 50 ps. We can implement DPS-QKD with a temporal multiplexed single photon detector. We further demonstrate that temporal filtering can reduce the QBER of our DPS-QKD implementation, but at a reduced secure key rate.

II. EXPERIMENTAL SETUP

In the first DPS-QKD proposal, a single photon was allowed to pass through a beam splitter, travel through different path delays and then recombined to create a superposition state of the photon [6]. However, this scheme would encounter beam splitter losses and reduces the secure key rate. The more common version of DPS-QKD is one that uses weak coherent pulses (WCPs) [19]. With a path superposition of N -paths, and a relative phase of $\{0, \pi\}$ between paths, the photon can be in a superposition of 2^{N-1} states. Similar states can also be achieved with time-bin superposition by adding a relative phase at $N-1$ locations within a single pulse. In this article, we define 2^{N-1} as M , and hence, refer to the 3-pulse DPS-QKD

Gautam Shaw is with the Department of Electrical Engineering, Indian Institute of Technology, Madras, e-mail: ee15d047@ee.iitmadras.ac.in.

as a 4-state system. This notation will allow us to describe the creation of superposition states by temporal phase modulation.

We describe our experiments with 4-state DPS-QKD, using space and time-bin superposition of a weak coherent source, as shown in Fig. 1. The time-bin superposition scheme is easier to implement and control, and can be extended to an M -state DPS-QKD scheme without any additional hardware complexity. When we use a superposition of 4 states, an intercept and resend (IR) attack by Eve introduces a 33% error on the sifted key. We had previously reported that the 4-state DPS scheme is more secure against both IR and beam splitter attacks [20]. This percentage error increases to 50% when 4-state DPS is extended to M -state DPS, but with ideal detectors [20]. The methodology used to implement a weak

Eve's intercept and resend attack introduces an error of 33% in the sifted key in the 4-state DPS compared to the 25% error when using a train of WCPs in conventional DPS-QKD.

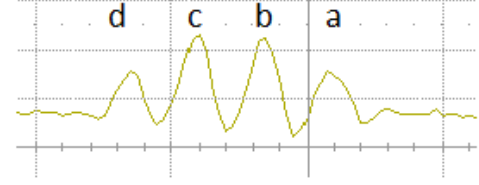


Fig. 2: Photodetector output after Alice's path superposition and Bob's DLI, captured with a diode laser source. The key is generated by the interference in time-bins b and c .

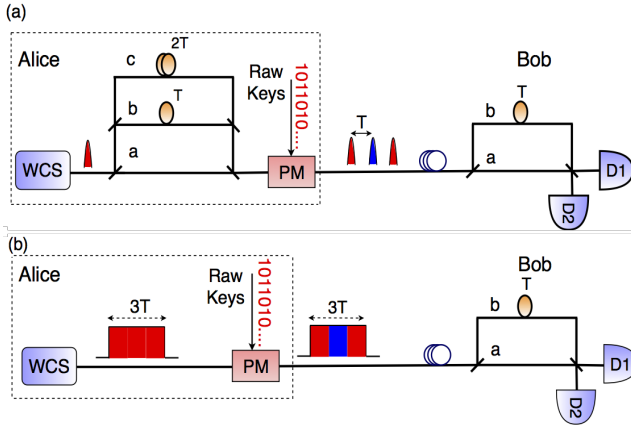


Fig. 1: 4-state DPS-QKD schemes using (a) spatial and (b) time-bin superposition with a weak coherent source. WCS: Weak coherent source, PM: phase modulator, T: time, D1 and D2: single photon detectors.

coherent source (WCS) is described along with the rest of our experimental setup in Sec. IV-A.

III. KEY GENERATION IN DPS-QKD

In our 4-state DPS-QKD implementation. Alice sends a single photon in a superposition of 3 spatial paths to Bob. The probability of a photon traveling through one of the 3 paths in Alice's set-up is $1/3$. The superposition state generated from Alice is represented as:

$$|\Psi\rangle = \frac{1}{\sqrt{3}} \left[|1\rangle_a |0\rangle_b |0\rangle_c \pm |0\rangle_a |1\rangle_b |0\rangle_c \pm |0\rangle_a |0\rangle_b |1\rangle_c \right] \quad (1)$$

$$\triangleq \frac{1}{\sqrt{3}} \left[|100\rangle_{abc} \pm |010\rangle_{abc} \pm |001\rangle_{abc} \right] \quad (2)$$

where the paths a , b , c also represent time-bins. $|\Psi\rangle$ is passed through a delay line interferometer (DLI) at Bob's site. As a result, the photon is now in a superposition of 4 time-bins. The first and last time-bins do not contain encoded phase difference information, whereas the 2 central time-bins contribute to the key generation. The 4 time-bins can also be observed classically, but at higher photon numbers, as shown in Fig. 2. Alice now encodes her random key bit as a random phase $\phi = \{0, \pi\}$ between successive time-bins. Bob extracts the key information using a DLI and two single-photon detectors.

The secure key rate (R_{sec}) is estimated from sifted key rate (R_{sifted}) as

$$R_{\text{sec}} = R_{\text{sifted}} [\tau - f(e)h(e)], \quad (3)$$

where τ is the shrinking factor, $f(e)$ captures the inefficiency of the error correcting code, and $h(e)$ is the binary Shannon entropy. The error rate, e , depends upon dark counts and other system imperfections and τ captures Eve's knowledge of the key. If we assume Eve's attack to be limited to the IR and beamsplitter attacks, increasing N changes the efficacy of the attacks, thus making τ a function of N [20]. Hence, a secure key rate that depends on both R_{sifted} and τ , varies with N as shown in Fig. 3.

Experimentally, the generation of a superposition state can be realized spatially using passive beam splitters (or beam combiners). However, passive beam splitters have insertion losses and the sifted key rate is reduced by a factor of N , thus making the implementation inefficient. An implementation with $N = 3$ will create $M = 4$ non-orthogonal states that Alice uses to transmit the key. Keeping in mind the ease of implementing time-bin superposition, we advocate temporal bins using phase modulation, over different spatial paths. This would potentially allow us to use $N > 3$ and obtain a higher sifted key rate, as seen in Fig. 3. However, with non-ideal SPDs, the optimal value against all attacks is $N = 3$ [11]. We observe this by the increase in QBER due to afterpulsing, within the same gate pulse, as N increases [21].

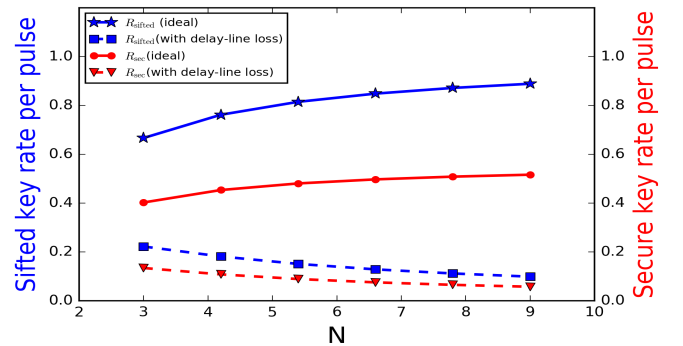


Fig. 3: Estimates for the sifted and secure key rate for M -state DPS-QKD, with ideal detectors.

the control parameters of the SPD, we were able to observe a QBER of 0.12, shown pictorially in Fig. 7(a), in the time-bin scheme.

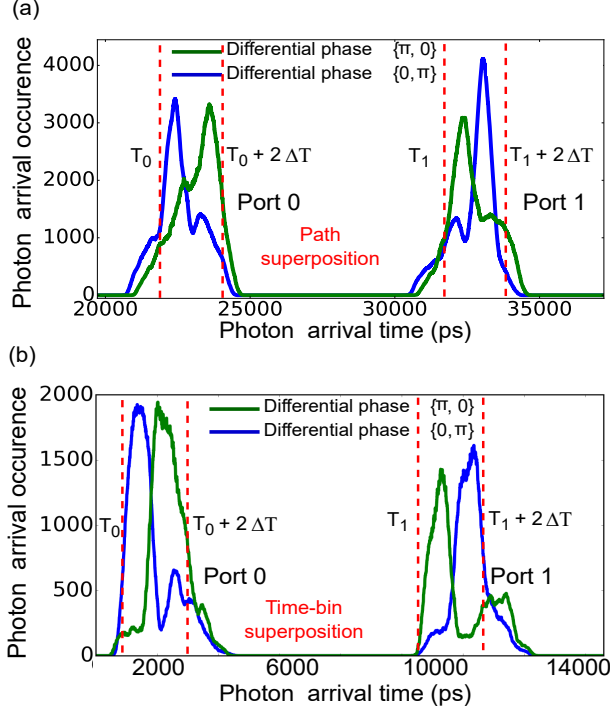


Fig. 6: Photon arrival time distribution for (a) path superposition and (b) time-bin superposition

With reference to Figs. 6 (a) and (b), the QBER is defined as,

$$\text{QBER} = \frac{C_{01} + C_{10}}{C_{00} + C_{10} + C_{01} + C_{11}} \quad (4)$$

where

$$C_{pq} = \sum_{t=T_{\text{start}}}^{T_{\text{stop}}} c_t \quad (5)$$

represents the counts at the p^{th} port of the DLI, when Alice's transmitted raw key is q . T_{start} and T_{stop} are determined for each case from Table. I.

TABLE I: Classification of photon counts

Phase pattern	C_{pq}	T_{start}	T_{stop}
{0, 0}	C_{00}	T_0	$T_0 + 2\Delta T$
	C_{01}	---	---
	C_{10}	T_1	$T_1 + 2\Delta T$
	C_{11}	---	---
	C_{00}	T_0	$T_0 + \Delta T$
{0, π }	C_{01}	$T_0 + \Delta T$	$T_0 + 2\Delta T$
	C_{10}	T_1	$T_1 + \Delta T$
	C_{11}	$T_1 + \Delta T$	$T_1 + 2\Delta T$
	C_{00}	$T_0 + \Delta T$	$T_0 + 2\Delta T$
	C_{01}	T_0	$T_0 + \Delta T$
{ π , 0}	C_{10}	$T_1 + \Delta T$	$T_1 + 2\Delta T$
	C_{11}	T_1	$T_1 + \Delta T$
	C_{00}	---	---
	C_{01}	T_0	$T_0 + 2\Delta T$
	C_{10}	---	---
{ π , π }	C_{11}	T_1	$T_1 + 2\Delta T$

We recovered the sifted key and extracted the QBER by directly comparing the sender's keys with the receiver's. This approach was used to optimize the RF delay and appropriately insert a phase shift every 1 ns within the 3 ns optical pulse, using a fixed pattern of $\{0, \pi\}$. Although the phase pattern was fixed, with a low mean photon number, channel loss, and a detector efficiency $\eta \sim 0.1$, we only detect a random bit pattern after the delay line interferometer.

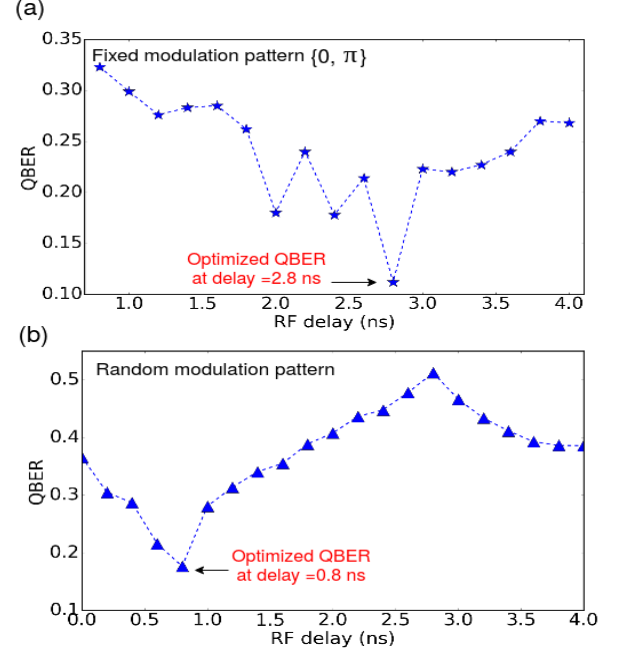


Fig. 7: Optimization of QBER by adjusting the timing of the applied phase (a) with fixed phase modulation pattern (b) with random phase modulation pattern

The QKD testbed was also used to investigate the effect of excess bias voltage, gate width and hold-off time on the dark count rate (DCR) and afterpulse noises of a gated InGaAs single-photon detector (SPD) [21]. This helped in improving the QBER for all 4 possible phase modulation patterns. We achieved a QBER of 0.12 for a fixed phase pattern $\{0, \pi\}$, as shown in Fig. 7 (a). Other patterns $\{0, 0\}$, $\{\pi, 0\}$ and $\{\pi, \pi\}$ yielded a QBER of 0.9, 0.14 and 0.27 respectively, while a random pattern yielded a minimum QBER of 0.17 as shown in Fig. 7(b).

The sifted key generation rate in our time-bin superposition DPS system can be written as [22]

$$R_{\text{sifted}} = r_p \mu \eta T_L e^{(-r_p \mu \eta T_L \tau_H)} \quad (6)$$

where the variables used are defined in Table II.

T_L consists of fiber loss due to attenuation ($\alpha \approx 0.2$ dB/km) and the net insertion loss (I_L) of the DLI and coupler. Referring to (6), the values of r_p , η and τ_H are 62.5 Mbps, 10% and 10 μs respectively. The exponential term in (6) approaches 1 for a transmitted pulse rate of 62.5 Mbps, with a hold-off time of 10 μs , and R_{sifted} decreases linearly with distance. However, the exponent becomes significant for higher transmitted pulse rates, typically $r_p > 1$ Gbps.

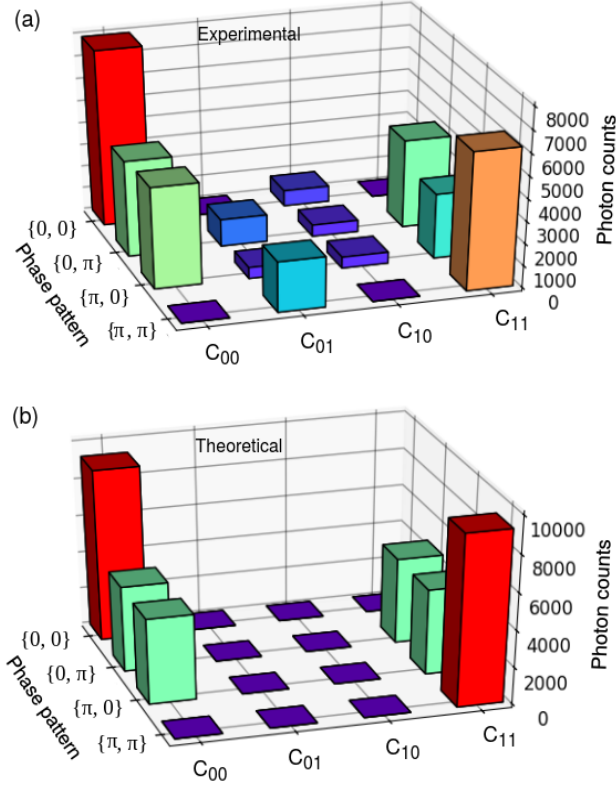


Fig. 8: Time-bin based differential-phase decoding by collecting photon arrival time for all four phase modulation states (a) experimental measurement (b) theoretical estimation

TABLE II: Variables used in sifted key rate (6)

Variables	Description
r_p	Pulse repetition rate
α	Attenuation constant of a single mode fiber
μ	Mean photon number per pulse
T_L	$10^{-\left(\frac{\alpha L + I_L}{10}\right)}$ (overall transmission efficiency of quantum channel)
η	Detection efficiency of SPD
T_{hold}	Hold-off time of SPD

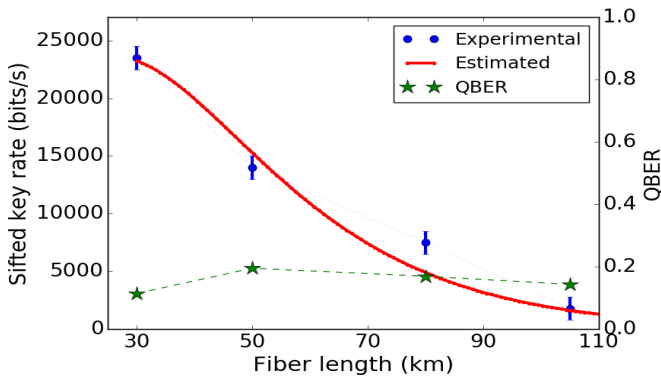


Fig. 9: Sifted key rate (estimated and experimental) and measured QBER as a function of channel length

As we observe in Fig. 9, the experimental data fits well to (6), and we estimate $\mu \approx 0.17$. At a fiber length of 30 km, we achieved a sifted key generation rate of 21 kbps with a QBER of 11.5 %. We then extended our experiment to 105 km of fiber, and observed the sifted key rate drop to about 2 kbps with a QBER of 14.4 %, as shown in Fig. 9.

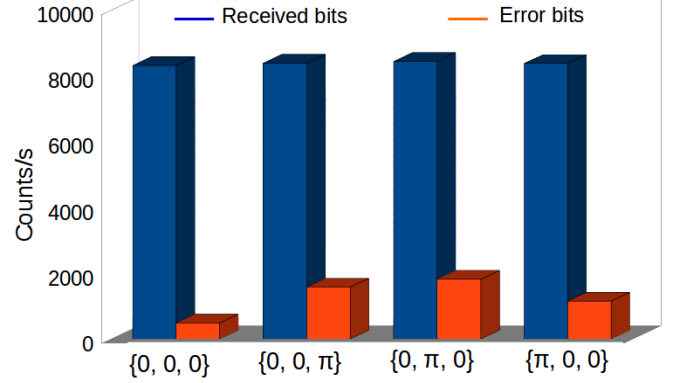


Fig. 10: Differential phase decoding in 8-state DPS-QKD. QBER for transmitted phase modulation states $\{0, 0, 0\}$, $\{0, 0, \pi\}$, $\{0, \pi, 0\}$ and $\{\pi, 0, 0\}$ are 0.06, 0.20, 0.22 and 0.14 respectively

We further extended our 4-state DPS experiments to realize 8-state DPS, with a DLI having free spectral range of 2.5 GHz. The phase modulation transition rate was enhanced from 1 GHz to 2.5 GHz within a photon wave packet of width 1.6 ns, where each time-bin size is 0.4 ns. Based on the photon arrival time within 1.2 ns, the QBER was calculated for various phase modulation states, as shown in Fig. 10.

B. Temporal filtering of time-stamps

After identification of the optimized gate and RF delay, we introduce a guard window between time-bins at the output state of Bob's set-up [23]. In temporal filtering, while we discard the time-stamps collected at the selected guard time, we lose a fraction of bits in sifted keys. However, this method reduces the QBER of a system [24], but at a cost of a reduced sifted key rate, as shown in Fig. 11 (a) and (b). Table III lists the source of errors, contributing in QBER for our QKD test-bed. Error due to DCR, afterpulse probability and timing jitter were estimated from our previous work on gated SPD characterization [25]. The interferometric visibility (V) of

TABLE III: Potential sources of errors in QKD test-bed

Description	Source	Error contribution (%)	
		$\Delta T = 1$ ns	$\Delta T = 0.4$ ns
Dark count rate (DCR)	SPD	0.33	0.33
Afterpulse effect	SPD	1.5	1.5
Extinction ratio	IM	1.6	1.6
Timing jitter	SPD	5.0	12.5
Imperfect visibility	DLI	4.0	2.0
Rise/fall time of PM pattern*	PM	2.1	5.25

* From data sheet.

two DLI with FSR of 1 GHz and 2.5 GHz are 92% and 96% respectively. The QBER introduced into the system due to

V is $(1 - V)/2$. Referring to Table III, the major sources of QBER are timing jitter of SPD and phase modulation rise/fall time, which can be reduced by temporal filtering method. For a guard time of 200 ps, 20 % key bits are discarded, while the QBER is reduced from 0.12 to 0.09 in a system with a DLI of FSR 1 GHz, as shown in Fig. 11 (a). For a DLI with 2.5 GHz FSR, we discard 20 % key bits, to reduce QBER from 0.14 to 0.12, as shown in Fig. 11 (b). The reduction in QBER for a larger FSR is only marginal. This highlights the challenge of moving to a DLI with a higher FSR. After estimating and

our time-bin superposition based DPS-QKD system to 105 km of optical fibre, and achieved a sifted key rate of 2 kbps while maintaining a QBER of 0.14. We also applied temporal filtering method in our DPS-QKD system, and shown that it helps to reduce the QBER, back to 0.12, but at a cost of reduced sifted key rate.

ACKNOWLEDGMENT

This work was supported by Ministry of Human Resources and Development (MHRD) vide sanction no. 35-8/2017-TS.

APPENDIX

TABLE IV: Decoy state implementations [27–29]

Author, Year	Protocol	Encoding scheme	Channel length	Key rate bits/s
Frohlich et al., 2017	BB84	Phase	240 km	8.4
Boaron et al., 2018	Simplified BB84	Time-bin	421 km	6.5
Yuan et al., 2018	BB84 variant	Phase	10 km	13.7 M

TABLE V: Measurement-device-independent (MDI) QKD implementations [30–37]

Author, Year	Protocol	Encoding scheme	Channel length	Key rate bits/s
Yin et al., 2016	Decoy state MDI	Time-bin	404 km	0.00032
Tang et al., 2016	BB84	Polarisation	40 km	10
Comandar et al., 2016	BB84	Polarisation	102 km	4.6 K
Wang et al., 2016	RFI [†]	Time-bin	20 km	0.0063
Valivarthi et al., 2017	BB84	Time-bin	80 km	100
Liu et al., 2019	BB84	Time-bin	160 km	2.6
Wei et al., 2020	Asymmetric MDI	Polarization	180 km	31
Zhou, et al., 2021	RFI [†]	Time-bin	200 km	1

[†] Reference-frame-independent.

TABLE VI: Twin-field (TF) QKD implementations [38–44]

Author, Year	Protocol	Encoding scheme	Channel length	Key rate bits/s
Minder et al., 2019	TF	Phase	90.8 dB	0.045
Wang et al., 2019	SNS-TF ^{††}	Time-bin	300 km	2.01 K
Liu et al., 2019	TF	Time-bin	300 km	39.2
Zhong et al., 2019	TF	Phase	55.1 dB	25.6
Fang et al, 2020	TF	Phase	502 km	0.118
Liu, Hui, et al, 2021	SNS-TF ^{††}	Time-bin	428 km	3.36
Wang, et al, 2021	TF	Phase	830 km	0.01

^{††} Sending-or-not-sending twin-field.

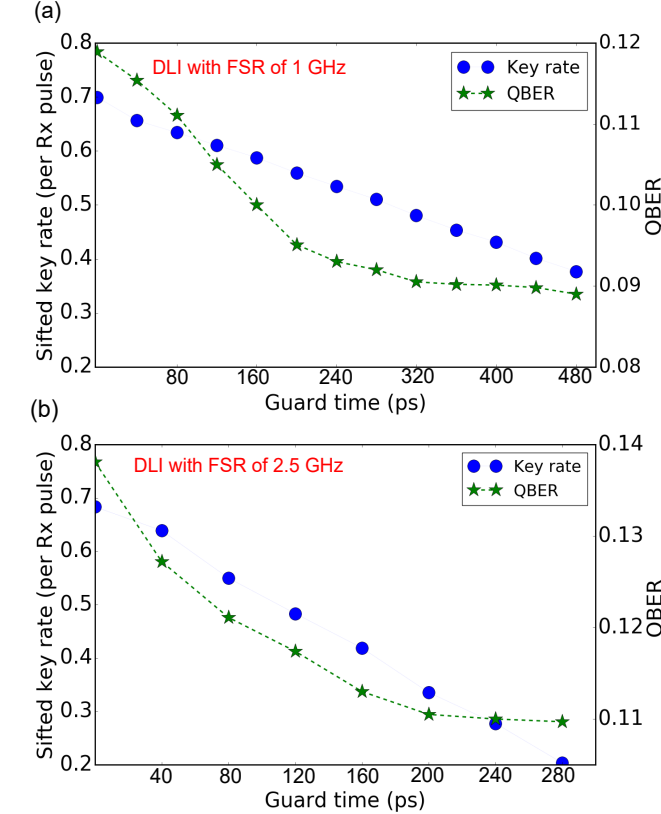


Fig. 11: Effect of temporal filtering on sifted key rate and QBER, (a) with DLI of FSR 1 GHz (b) with DLI of FSR 2.5 GHz. At higher guard time, QBER reduces at a cost of reduced sifted key rate per R_x detection.

optimizing QBER, we followed error correction and privacy amplification to generate secure keys. However, our focus is on QBER measurement and sifted key generation, hence error correction [26] and privacy amplification are not discussed in this paper.

VI. CONCLUSION AND PERSPECTIVES

We have presented two different experimental approaches (a) spatial superposition and (b) time-bin superposition, to realize a 4-state DPS-QKD over a 105 km quantum channel. We observe that the time-bin superposition scheme is more efficient and easier to implement and can be extended to an M -state DPS-QKD system. After optimization of various parameters, we achieved a sifted key rate of around 21 kbps with QBER of 0.12 over 30 km of fiber. We then extended

REFERENCES

- [1] N. Gisin, G. Ribordy, W. Tittel, and H. Zbinden, “Quantum cryptography,” *Reviews of Modern Physics*, vol. 74, no. 1, p. 145, 2002.
- [2] C. H. Bennett and G. Brassard, “Quantum cryptography: Public key distribution and coin tossing,” 1984.
- [3] Y. Liu, T.-Y. Chen, J. Wang, W.-Q. Cai, X. Wan, L.-K. Chen, J.-H. Wang, S.-B. Liu, H. Liang, L. Yang *et al.*, “Decoy-state quantum key distribution with polarized photons over 200 km,” *Optics Express*, vol. 18, no. 8, pp. 8587–8594, 2010.

TABLE VII: Continuous variable-QKD [45–47]

Author, Year	Protocol	Encoding scheme	Channel length	Key rate bits/s
Wang et al., 2017	CV	Gaussian modulation	50 km	700
Zhang et al., 2019	CV	Gaussian modulation	50 km	5800
Zhang et al., 2020	CV	Gaussian modulation	202.8 km	6.2

- [4] D. Stucki, S. Fasel, N. Gisin, Y. Thoma, and H. Zbinden, “Coherent one-way quantum key distribution,” in *Photon Counting Applications, Quantum Optics, and Quantum Cryptography*, vol. 6583. International Society for Optics and Photonics, 2007, p. 65830L.
- [5] A. K. Ekert, “Quantum cryptography based on Bell’s theorem,” *Physical Review Letters*, vol. 67, no. 6, p. 661, 1991.
- [6] K. Inoue, E. Waks, and Y. Yamamoto, “Differential phase shift quantum key distribution,” *Physical Review Letters*, vol. 89, no. 3, p. 037902, 2002.
- [7] S. Wang, W. Chen, Z.-Q. Yin, H.-W. Li, D.-Y. He, Y.-H. Li, Z. Zhou, X.-T. Song, F.-Y. Li, D. Wang et al., “Field and long-term demonstration of a wide area quantum key distribution network,” *Optics Express*, vol. 22, no. 18, pp. 21 739–21 756, 2014.
- [8] K. Inoue and T. Honjo, “Robustness of differential-phase-shift quantum key distribution against photon-number-splitting attack,” *Physical Review A*, vol. 71, no. 4, p. 042305, 2005.
- [9] C. H. Bennett, F. Bessette, G. Brassard, L. Salvail, and J. Smolin, “Experimental quantum cryptography,” *Journal of Cryptology*, vol. 5, no. 1, pp. 3–28, 1992.
- [10] E. Waks, H. Takesue, and Y. Yamamoto, “Security of differential-phase-shift quantum key distribution against individual attacks,” *Physical Review A*, vol. 73, no. 1, p. 012344, 2006.
- [11] K. Wen, K. Tamaki, and Y. Yamamoto, “Unconditional security of single-photon differential phase shift quantum key distribution,” *Physical Review Letters*, vol. 103, no. 17, p. 170503, 2009.
- [12] Y. Hui, Z. Shi-Liang, and D. Sheng-Wang, “Efficient phase-encoding quantum key generation with narrow-band single photons,” *Chinese Physics Letters*, vol. 28, no. 7, p. 070307, 2011.
- [13] C. Liu, S. Zhang, L. Zhao, P. Chen, C.-H. Fung, H. Chau, M. Loy, and S. Du, “Differential-phase-shift quantum key distribution using heralded narrow-band single photons,” *Optics Express*, vol. 21, no. 8, pp. 9505–9513, 2013.
- [14] A. Boaron, B. Korzh, R. Houlmann, G. Boso, D. Rusca, S. Gray, M.-J. Li, D. Nolan, A. Martin, and H. Zbinden, “Simple 2.5 GHz time-bin quantum key distribution,” *Applied Physics Letters*, vol. 112, no. 17, p. 171108, 2018.
- [15] I. Vagniluca, B. Da Lio, D. Rusca, D. Cozzolino, Y. Ding, H. Zbinden, A. Zavatta, L. K. Oxenløwe, and D. Bacco, “Efficient time-bin encoding for practical high-dimensional quantum key distribution,” *Physical Review Applied*, vol. 14, no. 1, p. 014051, 2020.
- [16] L. Dellantonio, A. S. Sørensen, and D. Bacco, “High-dimensional measurement-device-independent quantum key distribution on two-dimensional subspaces,” *Physical Review A*, vol. 98, no. 6, p. 062301, 2018.
- [17] J.-Y. Guan, Z. Cao, Y. Liu, G.-L. Shen-Tu, J. S. Pelc, M. Fejer, C.-Z. Peng, X. Ma, Q. Zhang, and J.-W. Pan, “Experimental passive round-robin differential phase-shift quantum key distribution,” *Physical Review Letters*, vol. 114, no. 18, p. 180502, 2015.
- [18] W. Qu, H. Liu, J. Wang, and H. Ma, “Adjustable round-pulse time delay for round-robin differential phase-shift quantum key distribution,” *Optics Communications*, vol. 448, pp. 43 – 47, 2019.
- [19] K. Inoue, E. Waks, and Y. Yamamoto, “Differential-phase-shift quantum key distribution using coherent light,” *Physical Review A*, vol. 68, no. 2, p. 022317, 2003.
- [20] S. K. Ranu, G. K. Shaw, A. Prabhakar, and P. Mandayam, “Security with 3-pulse differential phase shift quantum key distribution,” in *2017 IEEE Workshop on Recent Advances in Photonics (WRAP)*. IEEE, 2017, pp. 1–7.
- [21] G. Shaw, S. Sridharan, and A. Prabhakar, “Gated InGaAs detector characterization with sub-picosecond weak coherent pulses,” *Optik*, vol. 250, p. 168280, 2022.
- [22] E. Diamanti, H. Takesue, C. Langrock, M. Fejer, and Y. Yamamoto, “100 km differential phase shift quantum key distribution experiment with low jitter up-conversion detectors,” *Optics Express*, vol. 14, no. 26, pp. 13 073–13 082, 2006.
- [23] G. Shaw, S. Shyam, and A. Prabhakar, “Optimal temporal filtering for COW-QKD,” *IEEE International Conference on Signal Processing and Communications (SPCOM)*, Paper ID: 362, 2022.
- [24] T. Kupko, M. von Helversen, L. Rickert, J.-H. Schulze, A. Strittmatter, M. Gschrey, S. Rodt, S. Reitzenstein, and T. Heindel, “Tools for the performance optimization of single-photon quantum key distribution,” *npj Quantum Information*, vol. 6, no. 1, pp. 1–8, 2020.
- [25] G. Shaw, S. Shyam, S. Foram, S. Ranu, P. Mandayam, and A. Prabhakar, “3 pulse differential phase shift quantum key distribution with spatial, or time, multiplexed,” in *Laser Science*. Optical Society of America, 2019, pp. JW3A–54.
- [26] A. K. Pradhan, A. Thangaraj, and A. Subramanian, “Construction of near-capacity protograph ldpc code sequences with block-error thresholds,” *IEEE Transactions on Communications*, vol. 64, no. 1, pp. 27–37, 2015.
- [27] A. Boaron, G. Boso, D. Rusca, C. Vulliez, C. Autebert, M. Caloz, M. Perrenoud, G. Gras, F. Bussi eres, M.-J. Li et al., “Secure quantum key distribution over 421 km of optical fiber,” *Physical Review Letters*, vol. 121, no. 19, p. 190502, 2018.
- [28] Z. Yuan, A. Plews, R. Takahashi, K. Doi, W. Tam, A. Sharpe, A. Dixon, E. Lavelle, J. Dynes, A. Murakami et al., “10-mb/s quantum key distribution,” *Journal of Lightwave Technology*, vol. 36, no. 16, pp. 3427–3433, 2018.
- [29] B. Fr hlich, M. Lucamarini, J. F. Dynes, L. C. Comandar, W. W.-S. Tam, A. Plews, A. W. Sharpe, Z. Yuan, and A. J. Shields, “Long-distance quantum key distribution secure against coherent attacks,” *Optica*, vol. 4, no. 1, pp. 163–167, 2017.
- [30] H.-L. Yin, T.-Y. Chen, Z.-W. Yu, H. Liu, L.-X. You, Y.-H. Zhou, S.-J. Chen, Y. Mao, M.-Q. Huang, W.-J. Zhang et al., “Measurement-device-independent quantum key distribution over a 404 km optical fiber,” *Physical Review Letters*, vol. 117, no. 19, p. 190501, 2016.
- [31] Z. Tang, K. Wei, O. Bedrova, L. Qian, and H.-K. Lo, “Experimental measurement-device-independent quantum key distribution with imperfect sources,” *Physical Review A*, vol. 93, no. 4, p. 042308, 2016.
- [32] L. Comandar, M. Lucamarini, B. Fr hlich, J. Dynes, A. Sharpe, S.-B. Tam, Z. Yuan, R. Pentty, and A. Shields, “Quantum key distribution without detector vulnerabilities using optically seeded lasers,” *Nature Photonics*, vol. 10, no. 5, p. 312, 2016.
- [33] C. Wang, Z.-Q. Yin, S. Wang, W. Chen, G.-C. Guo, and Z.-F. Han, “Measurement-device-independent quantum key distribution robust against environmental disturbances,” *Optica*, vol. 4, no. 9, pp. 1016–1023, 2017.
- [34] R. Valivarthi, Q. Zhou, C. John, F. Marsili, V. B. Verma, M. D. Shaw, S. W. Nam, D. Oblak, and W. Tittel, “A cost-effective measurement-device-independent quantum key distribution system for quantum networks,” *Quantum Science and Technology*, vol. 2, no. 4, p. 04LT01, 2017.
- [35] H. Liu, W. Wang, K. Wei, X.-T. Fang, L. Li, N.-L. Liu, H. Liang, S.-J. Zhang, W. Zhang, H. Li et al., “Experimental demonstration of high-rate measurement-device-independent quantum key distribution over asymmetric channels,” *Physical Review Letters*, vol. 122, no. 16, p. 160501, 2019.
- [36] K. Wei, W. Li, H. Tan, Y. Li, H. Min, W.-J. Zhang, H. Li, L. You, Z. Wang, X. Jiang et al., “High-speed measurement-device-independent quantum key distribution with integrated silicon photonics,” *Physical Review X*, vol. 10, no. 3, p. 031030, 2020.
- [37] X.-Y. Zhou, H.-J. Ding, M.-S. Sun, S.-H. Zhang, J.-Y. Liu, C.-H. Zhang, J. Li, and Q. Wang, “Reference-frame-independent measurement-device-independent quantum key distribution over 200 km of optical fiber,” *Physical Review Applied*, vol. 15, no. 6, p. 064016, 2021.
- [38] M. Minder, M. Pittaluga, G. Roberts, M. Lucamarini, J. Dynes, Z. Yuan, and A. Shields, “Experimental quantum key distribution beyond the repeaterless secret key capacity,” *Nature Photonics*, vol. 13, no. 5, pp. 334–338, 2019.
- [39] S. Wang, D.-Y. He, Z.-Q. Yin, F.-Y. Lu, C.-H. Cui, W. Chen, Z. Zhou, G.-C. Guo, and Z.-F. Han, “Beating the fundamental rate-distance limit in a proof-of-principle quantum key distribution system,” *Physical Review X*, vol. 9, no. 2, p. 021046, 2019.
- [40] Y. Liu, Z.-W. Yu, W. Zhang, J.-Y. Guan, J.-P. Chen, C. Zhang, X.-L. Hu, H. Li, C. Jiang, J. Lin et al., “Experimental twin-field quantum key distribution through sending or not sending,” *Physical Review Letters*, vol. 123, no. 10, p. 100505, 2019.
- [41] X. Zhong, J. Hu, M. Curty, L. Qian, and H.-K. Lo, “Proof-of-principle experimental demonstration of twin-field type quantum key distribution,” *Physical Review Letters*, vol. 123, no. 10, p. 100506, 2019.
- [42] X.-T. Fang, P. Zeng, H. Liu, M. Zou, W. Wu, Y.-L. Tang, Y.-J.

- Sheng, Y. Xiang, W. Zhang, H. Li *et al.*, “Implementation of quantum key distribution surpassing the linear rate-transmittance bound,” *Nature Photonics*, pp. 1–4, 2020.
- [43] H. Liu, C. Jiang, H.-T. Zhu, M. Zou, Z.-W. Yu, X.-L. Hu, H. Xu, S. Ma, Z. Han, J.-P. Chen *et al.*, “Field test of twin-field quantum key distribution through sending-or-not-sending over 428 km,” *Physical Review Letters*, vol. 126, no. 25, p. 250502, 2021.
- [44] S. Wang, Z.-Q. Yin, D.-Y. He, W. Chen, R.-Q. Wang, P. Ye, Y. Zhou, G.-J. Fan-Yuan, F.-X. Wang, Y.-G. Zhu *et al.*, “Twin-field quantum key distribution over 830-km fibre,” *Nature Photonics*, pp. 1–8, 2022.
- [45] X. Wang, W. Liu, P. Wang, and Y. Li, “Experimental study on all-fiber-based unidimensional continuous-variable quantum key distribution,” *Physical Review A*, vol. 95, no. 6, p. 062330, 2017.
- [46] Y. Zhang, Z. Li, Z. Chen, C. Weedbrook, Y. Zhao, X. Wang, Y. Huang, C. Xu, X. Zhang, Z. Wang *et al.*, “Continuous-variable qkd over 50 km commercial fiber,” *Quantum Science and Technology*, vol. 4, no. 3, p. 035006, 2019.
- [47] Y. Zhang, Z. Chen, S. Pirandola, X. Wang, C. Zhou, B. Chu, Y. Zhao, B. Xu, S. Yu, and H. Guo, “Long-distance continuous-variable quantum key distribution over 202.81 km of fiber,” *Physical Review Letters*, vol. 125, no. 1, p. 010502, 2020.